Supporting Information

Oxidase-like Mimic of $Ag@Ag_3PO_4$ Microcubes as A Smart Probe for Ultrasensitive and Selective Hg^{2+} Detection

Dong-Feng Chai[a]‡, Zhuo Ma[b]‡, Yunfeng Qiu[c,d]*, Yu-Guang Lv,[a] Hong Liu[a]*, Chao-Yu Song[a], Guang-Gang Gao[a,e]*

[a] Department of Chemistry, College of Pharmacy, Jiamusi University, Jiamusi 154004, China. E-mail: hliu@jmsu.edu.cn (H. Liu) , gaogg@jmsu.edu.cn (G. Gao)

[b] School of Life Science and Technology, Harbin Institute of Technology, 92 West Dazhi Street, Harbin, Heilongjiang, 150001, China.

[c] State Key Laboratory of Urban Water Resource and Environment, Harbin Institute of Technology, Harbin 150090, China. E-mail: qiuyf@hit.edu.cn (Y. Qiu).

[d] State Key Laboratory of Robotics and System (HIT), Harbin, Heilongjiang 150080, China.

[e] Department of Chemistry, Changchun Normal University, Changchun, 130032, China.

‡ These authors contributed equally to this work.

Contents:

1) **Figure S1.** X-ray spectroscopy (EDS) analysis.

2) **Figure S2.** FTIR and Raman spectra of Ag_3PO_4MCs and Ag@Ag_3PO_4MCs.

3) **Figure S3.** The catalytic performances of Ag_3PO_4MCs for TMB in the presence of H_2O_2, O_2 and N_2.

4) **Figure S4.** Dependence of the oxidase-like activity of the TMB concentrations and catalysts amounts.

5) **Figure S5.** Dependence of the oxidase-like activity of pH values of buffer solutions and reaction temperature.

6) **Figure S6.** The catalytic performance of Ag_3PO_4MCs for OPD under different UV irradiation time. Inset is the relative activity versus irradiation time.

7) **Figure S7.** XPS of Ag@Ag_3PO_4MCs.

8) **Figure S8.** The mercury(II)-inhibited catalytic dynamics of Ag_3PO_4MCs or Ag@Ag_3PO_4MCs.

9) **Figure S9.** Steady-state kinetic assays of Ag_3PO_4MCs and Ag_3PO_4MCs with Hg^{2+} ions.

10) **Table S1.** Apparent kinetic parameters of different nanostructures.

11) **Table S2.** Comparison of assay methods for monitoring Hg^{2+} ions.

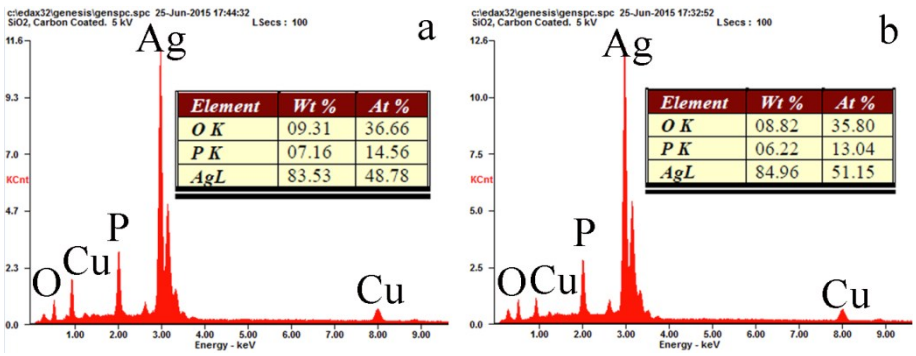

Figure S1. EDS of (a) Ag_3PO_4MCs and (b) Ag@ Ag_3PO_4MCs. Each sample was measured in three batches for data consistency.

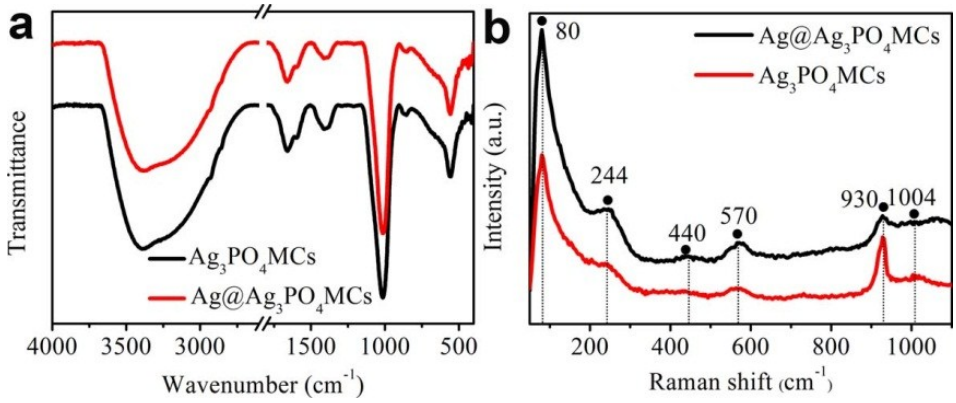

Figure S2. FTIR and Raman spectra of Ag_3PO_4MCs and $Ag@Ag_3PO_4MCs$.

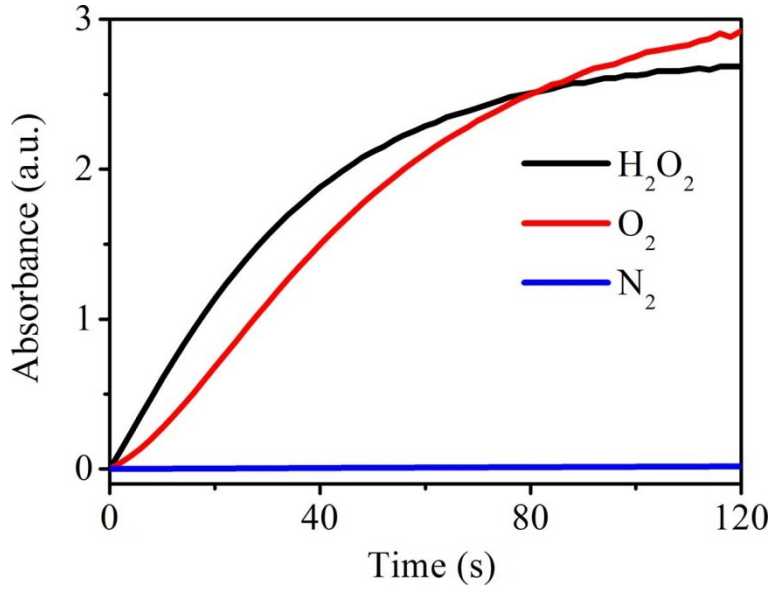

Figure S3. The catalytic performances of Ag_3PO_4MCs for TMB in the presence of H_2O_2, O_2 and N_2.

In order to have a deep understanding on the intrinsic oxidase-like properties of Ag_3PO_4MCs, systematic studies are performed on the effect of the TMB or OPD concentrations, catalysts amounts, pH values of buffer solutions, and reaction temperature. It has been well established that enzyme-reactions are dependent on all the above mentioned reaction parameters, such as horseradish peroxidase (HRP). Under our experimental conditions, various TMB or OPD concentrations were checked for better observation of UV-vis spectra measurement. As shown in Fig. S4a and S4c, 0.3 mM TMB or 1.25 mM OPD was found to be optimal to provide satisfied absorbance of UV-vis measurement, and the bluish or yellowish colour after reaction is clear to see by naked eyes. Meanwhile, 70 μg mL^{-1} Ag_3PO_4MCs was optimal to catalyze the oxidation reaction to equilibrium in a short time (120 s) in both cases of TMB and OPD in Fig. S4b and S4d. To evaluate the effects of pH values and reaction temperature on catalytic performance, the catalytic experiments in various pH values and reaction temperature have been carried out. In Fig. S5a, the relative activity was defined according to the absorption at 652 nm of the characteristic peak of oxidized TMB. It is clear to see that the relative activity of the Ag_3PO_4MCs gradually reached a maximum at pH value of 6.0 in 120 s, and decreased rapidly as increasing the pH to 6.8. Similar to previous work, the catalytic activity of most enzyme mimics is greatly affected by pH values. Ag_3PO_4MCs almost lost its oxidase-like activity at lower pH value around 3. As shown in Fig. S5b, Ag_3PO_4MCs exhibited higher catalytic activity at lower reaction temperature around 20 ^oC in the case of TMB, which lost its activity as increasing the reaction temperature. Similarly, using OPD as indicator also gives rise to the dependence on pH values in Fig. S5c. However, the absorption at 450 nm of oxidized OPD became maximal at pH value of 4.5, ascribing to different structural configuration of TMB and OPD. We observed different profiles using OPD as substrate as increasing reaction temperature, and Ag_3PO_4MCs shows the highest catalytic activity at 50 ^oC in Fig. S5d.

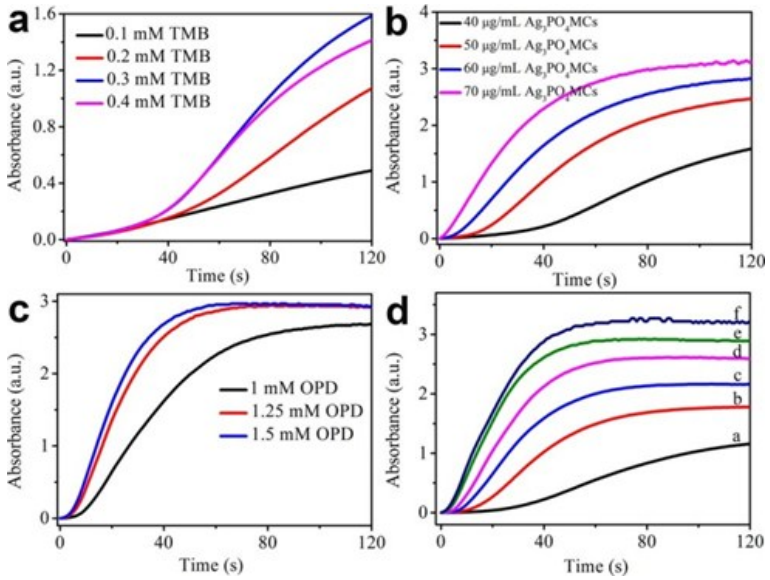

Figure S4. (a) Dependence of the oxidase-like activity on TMB concentrations. (b) Dependence of the oxidase-like activity on Ag_3PO_4MCs concentrations (by weight). (c) Dependence of the oxidase-like activity on OPD concentrations. (d) Dependence of the oxidase-like activity on the Ag_3PO_4MCs concentrations (a: 40 μg mL^{-1}, b: 50 μg mL^{-1}, c: 60 μg mL^{-1}, d: 70 μg mL^{-1}, e: 80 μg mL^{-1}, f: 90 μg mL^{-1}.). TMB experiments were conducted in time course mode in acetate buffer solution (pH = 6) at 20 °C. OPD experiments were conducted in time course mode in acetate buffer solution (pH = 4.5) at 50 °C.

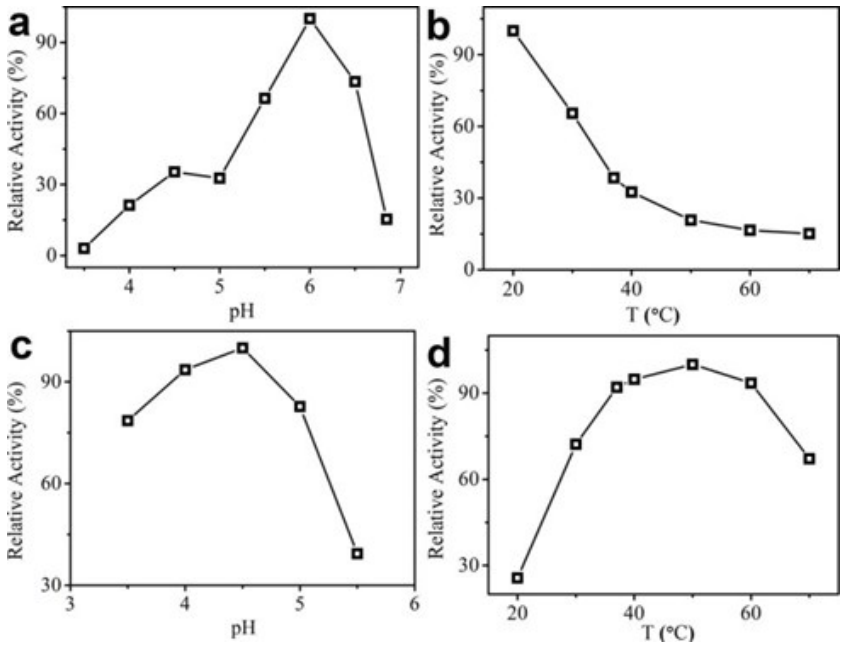

Figure S5. (a) (b) Dependence of the oxidase-like activity on the pH values (3.5, 4, 4.5, 5, 5.5, 6, 6.5, and 6.8), and reaction temperature (T) (20, 30, 37, 40, 50, 60, and 70 °C) using TMB as indicator. (c) (d) Dependence of the oxidase-like activity on the pH values (3.5, 4, 4.5, 5, and 5.5), and reaction temperature (T) (20, 30, 37, 40, 50, 60, and 70 °C) using OPD as indicator.

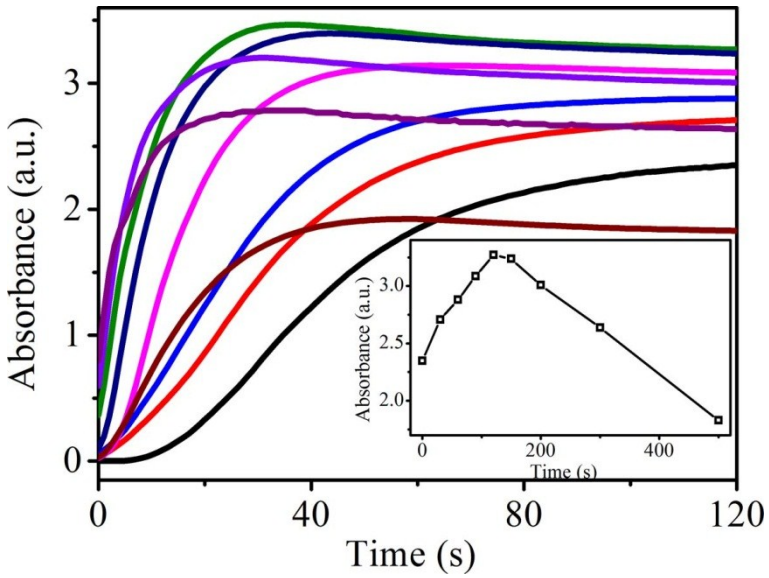

Figure S6. The catalytic performance of Ag_3PO_4MCs for OPD under different UV irradiation time. Inset is the relative activity versus irradiation time.

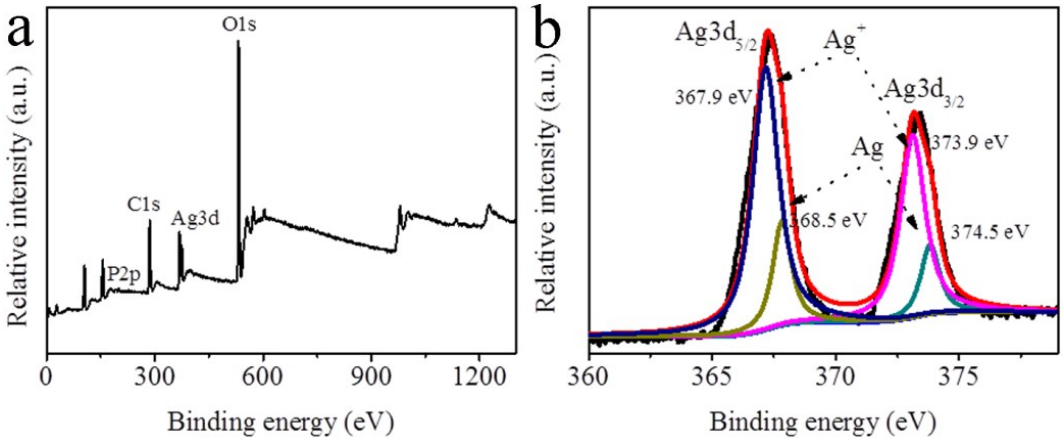

Figure S7. (a) XPS survey of $Ag@Ag_3PO_4MCs$, and (a) deconvoluted spectra of Ag 3d.

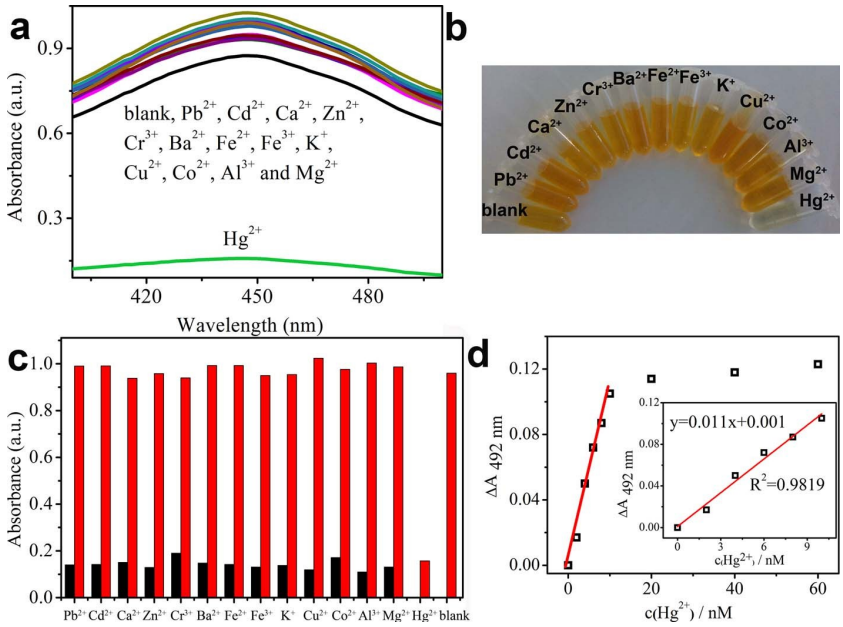

Figure S8. (a) The UV-vis spectra of Ag_3PO_4MCs/OPD solutions without and with addition of different metal ions (50 nM). (b) The photographs of Ag_3PO_4MCs/OPD solutions without and with addition of different metal ions (50 nM). (c) The absorbance values at 450 nm of Ag_3PO_4MCs/OPD solutions without and with addition of different metal ions; the red bars represent the cases of the addition of metal ions (50 nM), the black bars represent the cases of the addition of metal ions (250 nM) mixed with Hg^{2+} (50 nM). (d) Dose-response curve for Hg^{2+} detection based on inhibition reaction. Inset of d: linear calibration plot, absorbance change ΔA at 492 nm after addition of Ag_3PO_4MCs for 30 s *versus* Hg^{2+} concentrations. $\Delta A_{492\ nm} = A_0 - A_i$ (A_0 and A_i are the absorbance without Hg^{2+} and that with a Hg^{2+} concentration of i, respectively). Ag_3PO_4MCs/OPD solutions: [OPD] = 1.25 mM, [Ag_3PO_4MCs] = 150 μg mL^{-1} in 0.1 M, pH = 4.5 acetate buffer solution at 50 °C.

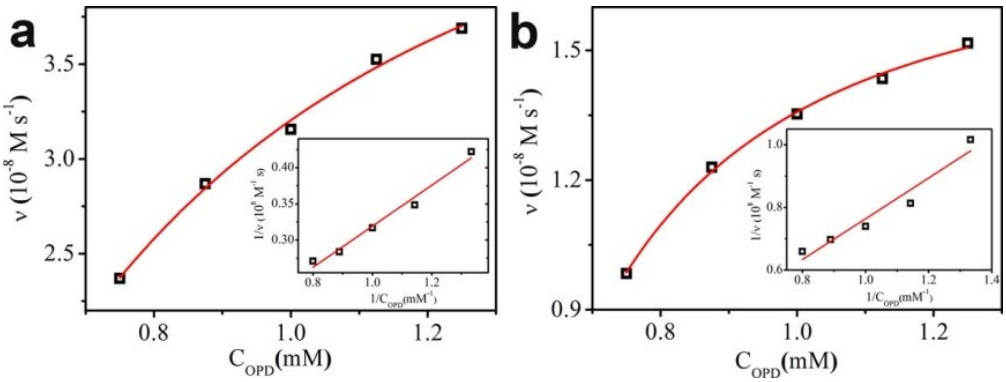

Figure S9. Steady-state kinetic assays of Ag_3PO_4MCs (70 μg mL^{-1}) with Hg^{2+} 50 nM (a) and Ag@Ag_3PO_4MCs (20 μg mL^{-1}) with Hg^{2+} 100 nM (b).

Table S1. Apparent kinetic parameters of different nanostructures. K_m is the Michaelis constant and V_{max} is the maximal reaction velocity.

Cat.	Substrate	K_m/mM	V_{max}/M s^{-1}	Ref.
HRP	OPD	0.59	4.65×10^{-8}	1
HRP	TMB	0.434	10×10^{-8}	2
Ag_3PO_4MCs	OPD	3.31	2.77×10^{-6}	This work
Ag@Ag_3PO_4MCs	OPD	1.23	5.18×10^{-6}	This work
Ag_3PO_4MCs	TMB	2.09	2.42×10^{-5}	This work
Ag@Ag_3PO_4MCs	TMB	0.11	6.32×10^{-6}	This work

Table S2. Comparison of assay methods for monitoring Hg^{2+} ions.

Strategy	Detection signal	Dynamic range (nM)	Detection limit (nM)	Ref.
Gel-AgNPs	colorimetric		0.125	3
L-tyrosine-AgNPs	colorimetric		16	4
AgNPs	colorimetric	16-660	16	4
Cit-AgNPs	colorimetric		28	5
Ag_3PO_4MCs	colorimetric	0-10	0.277	This work
Ag@Ag_3PO_4MCs	colorimetric	0-30	0.253	This work

References:

1. W.-Q. Kan, J. Yang, Y.-Y. Liu and J.-F. Ma, *Inorg. Chem.*, 2012, **51**, 11266.
2. L. Gao, J. Zhuang, L. Nie, J. Zhang, Y. Zhang, N. Gu, T. Wang, J. Feng, D. Yang, S. Perrett and X. Yan, *Nat. Nanotechnol.*, 2007, **2**, 577.
3. Z. Sun, N. Zhang, Y. Si, S. Li, J. Wen, X. Zhu and H. Wang, *Chem. Commun.*, 2014, **50**, 9196.
4. M. Annadhasan, T. Muthukumarasamyvel, V. R. Sankar Babu and N. Rajendiran, *ACS Sustain. Chem. Eng.*, 2014, **2**, 887.
5. G.-L. Wang, X.-F. Xu, L.-H. Cao, C.-H. He, Z.-J. Li and C. Zhang, *RSC Adv.*, 2014, **4**, 5867.